Child's Nervous System (2022) 38:33–50
https://doi.org/10.1007/s00381-021-05359-6

REVIEW ARTICLE

Neuroimaging of paediatric pineal, sellar and suprasellar tumours: a guide to differential diagnosis

Emma A. Lim[1,2] · César A. P. F. Alves[3] · Stefania Picariello[4] · Kristian Aquilina[5] · Sotirios Bisdas[2] · Ulrike Loebel[1] · Kshitij Mankad[1] · Felice D'Arco[1]

Received: 19 July 2021 / Accepted: 5 September 2021 / Published online: 16 September 2021
© The Author(s), under exclusive licence to Springer-Verlag GmbH Germany, part of Springer Nature 2021

Abstract

Introduction Pineal, sellar and suprasellar tumours in children comprise a wide range of diseases with different biological behaviours and clinical management. Neuroimaging plays a critical role in the diagnosis, treatment planning and follow up of these patients, but imaging interpretation can prove challenging due to the significant overlap in radiological features.

Materials and method A review of the literature was performed by undertaking a search of the MEDLINE and EMBASE databases for appropriate MeSH terminology. Identified abstracts were screened for inclusion and articles meeting the objectives of the review were included.

Results and Conclusion In this article, we review radiological appearances of common and uncommon pineal, sellar and suprasellar tumours occurring in the paediatric population. We discuss the importance of anatomical localization, clinical information and cerebrospinal fluid tumour markers, and propose a practical approach to differential diagnosis. Lastly, we discuss future directions and prospective new imaging strategies to support state-of-the-art patient care.

Keywords Brain tumours · Magnetic resonance imaging · Neuroimaging · Pineal gland · Sellar · Suprasellar

Introduction

Tumours of the central nervous system (CNS) constitute the largest group of solid neoplasms in children and are the leading cause of cancer mortality in the 0–14 age group [1]. Pineal, sellar and suprasellar tumours in children comprise a wide range of diseases with different biological behaviour and clinical management. Neuroimaging plays a critical role in the diagnosis, treatment planning and follow-up of these tumours, but image interpretation can be challenging. In this article, we review the radiological appearances of common and uncommon pineal, sellar and suprasellar tumours occurring in the paediatric population, and propose imaging protocols for clinical use (Tables 1 and 2).

✉ Emma A. Lim
emma.lim@nhs.net

1 Great Ormond Street Hospital for Children NHS Trust, Department of Radiology, London, UK

2 National Hospital for Neurology and Neurosurgery, Department of Radiology, London, UK

3 Department of Radiology, The Children's Hospital of Philadelphia, Philadelphia, PA, USA

4 Department of Women's and Children's Health, University of Campania Luigi Vanvitelli, Naples, IT , USA

5 Great Ormond Street Hospital for Children NHS Trust, Department of Neurosurgery, London, UK

Pineal region masses

Pineal region neoplasms constitute approximately 2.8–11% of brain tumours in children [2, 3], and are typically of primary pineal origin [4]. Primary pineal tumours may be divided into tumours of germ cell origin, tumours of pineal parenchymal origin and tumours of tissues adjacent to the pineal gland.

The clinical presentation is dependent on the location, size and aetiology of the lesion. Patients may present with obstructive hydrocephalus secondary to compression of the aqueduct and quadrigeminal plate, signs and symptoms related to brainstem compression, including vertical gaze disturbance, or endocrine and visual abnormalities secondary to synchronous tumour involvement of the pituitary gland, infundibulum or suprasellar region. When approaching the image interpretation of a pineal region mass in the paediatric patient, the age, diffusion characteristics and presence and distribution of multifocal disease are of critical importance.

Table 1 Suggested MRI protocol for pineal gland tumours

Essential sequences			
Pre-contrast sequence	**Technique**	**Parameters**	**Plane**
T1W	3D gradient echo (MPRAGE/IR SPGR/Fast SPGR/3D TFE/3D FFE)	Isotropic resolution Slice thickness ≤ 1 mm	Sagittal with axial and coronal reformats
T2W	TSE/FSE	≤ 4 mm	Axial and coronal
T2 FLAIR	TSE/FSE	≤ 4 mm	Axial and coronal
DWI	2D EPI	At least $b=0$ and 1000. ADC maps reconstructed < 4 mm	Axial
SWI/SWAN/T2*	GE	≤ 4 mm	Axial
Spine—cervical, thoracic and lumbar T2W[a]	TSE/FSE	≤ 4 mm	Sagittal and axial
Post-contrast Sequence	**Technique**	**Parameters**	**Plane**
T1W	TSE/FSE	≤ 4 mm	Axial
T1W	3D gradient echo (MPRAGE/IR SPGR/Fast SPGR/3D TFE/3D FFE)	Isotropic resolution Slice thickness ≤ 1 mm	Sagittal with axial and coronal reformats
Spine—cervical, thoracic and lumbar T1W post-contrast[a]	TSE/FSE	≤ 4 mm	Sagittal and axial
Complementary sequences and studies			
Sequence	**Technique**	**Parameters**	**Plane**
Heavily weighted T2W[b]	2D or 3D CISS/B FFE/FIESTA	Slice thickness ≤ 1 mm	Sagittal on the midline with axial and coronal reformats
CSF flow study[c]	Phase-contrast CSF flow	Velocity encoding gradient of 5	Sagittal
1H- MRS	Single vVoxel (**preferred**) Multi voxel	Short TE: 20–30 ms	3D voxel placed centred in the region of interest
ASL (2D or 3D)	**EPI** Pulsed Continuous Pseudocontinuous Velocity-selective	8.0 mm	Axial

[a]Necessary for pineal tumours with a high incidence of drop metastasis. For embryonal tumours, DWI sequence of the spine should be considered

[b]This sequence can also be applied for detailed analysis of drop metastasis affecting the spinal roots

[c]For analysis of CSF flow in the setting of a third ventriculostomy

Germ cell tumours

Germ cell tumours (GCTs) are the most common group of pineal region neoplasms [5, 6] and are typically midline in location. As detailed below, when symptomatic the clinical presentation is frequently related to mass effect on local structures in the pineal region, causing increased intracranial pressure. In the suprasellar region, symptoms often relate to endocrine disorders such as diabetes insipidus. Germ cell tumours can be categorised as germinomas or non-germinomatous germ cell tumours (nGGCTs) [7].

Germinoma

Germinomas are the most common pineal germ cell tumour [7, 8], with a peak incidence in the 10–19-year age group [9], declining significantly thereafter. Pineal germinomas demonstrate a strong male predominance [10], and the incidence is higher in the Japanese population [11]. As the target destination of germ cells is the primary reproductive organs, it is postulated that the intracranial location of GCTs may be secondary to aberrant migration of primordial germ cells [12]. Two types of intracranial germinoma are recognised: 'pure' germinoma and mixed germinomas containing components of other GCTs such as syncytiotrophoblastic giant cells; the latter being associated with beta-human chorionic gonadotropin (βHCG) secretion and a higher intracranial recurrence rate. In addition to the pineal region, germinomas may occur in the suprasellar cistern or, rarely, with an off-midline distribution including the basal ganglia, thalamus or cerebellum [9, 13]. Even more infrequently, they may primarily

Table 2 Suggested MRI protocol for sellar and suprasellar tumours

Essential sequences—standard brain MRI with contrast plus additional sequences[a]			
Pre-contrast sequence	**Technique**	**Parameters**	**Plane**
T1W	SE	≤ 3 mm	Sagittal and coronal
T2W	TSE/FSE	≤ 3 mm	Coronal
SWI/SWAN/T2*	GE	≤ 4 mm	Axial
Post-contrast sequence	**Technique**	**Parameters**	**Plane**
T1W delayed	3D gradient echo (MPRAGE/IR SPGR/Fast SPGR/3D TFE/3D FFE)	Isotropic resolution Slide thickness < 1 mm	Sagittal with axial and coronal reformats
Complementary sequences and studies			
Sequence	**Technique**	**Parameters**	**Plane**
Heavily weighted T2W[b]	2D or 3D CISS/B FFE/FIESTA	Slice thickness < 1 mm	Sagittal with axial and coronal reformats
T1W dynamic (for microadenomas only)	TSE/FSE Multiple time points (at least 6 recommended)	≤ 3 mm	Coronal
1H-MRS	Single voxel (**preferred**) Multi voxel	Short TE: 20–30 ms	3D voxel placed centred in the region of interest
Spine—cervical, thoracic and lumbar T1W post-contrast[c]	TSE/FSE	≤ 4 mm	Sagittal and axial
Spine—cervical, thoracic and lumbar T2W[c]	TSE/FSE	≤ 4 mm	Sagittal and axial

[a]Sequences with small FOV targeting the sellar and suprasellar region. Additional sequences of the orbits (coronal T2W and post-contrast T1W with fat saturation) should be considered for adequate coverage of tumours extending through the optic nerves and chiasm

[b]This sequence can also be applied for a detailed analysis of drop metastases affecting the spinal roots

[c]Necessary for sellar/suprasellar tumors with a high incidence of drop metastasis. For embryonal tumours, the DWI sequence of the spine should be considered

affect the spinal cord [14]. In 6–13% of cases, synchronous tumours are found in the pineal and suprasellar regions, termed a 'bifocal germinoma' [9]. Germinomas may invade local structures or disseminate throughout the cerebrospinal fluid (CSF).

The typical CT appearances are that of a hyperdense, midline mass centred on the pineal gland. In children, central physiological calcification of the gland is not usually observed until at least 4 years of age. Whilst not pathognomonic, a pattern of central, 'engulfed' calcification may be present, in contradistinction to the peripheral 'exploded' calcification typically associated with pineal parenchymal tumours [15] (Fig. 1a). On MRI, pineal germinomas are typically isointense to grey matter on T1WI, hypointense on T2WI and exhibit reduced ADC values (in keeping with high cellularity) (Fig. 1b, c). ADC values have been utilised

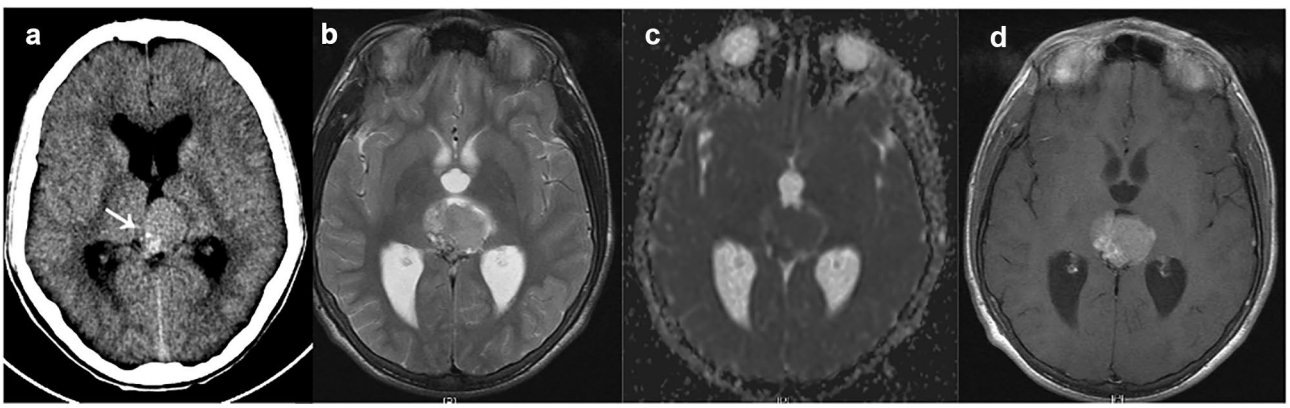

Fig. 1 Eight-year-old girl with a pineal germinoma: axial unenhanced CT (**a**) shows engulfed calcification in the posterior aspect of the pineal mass (arrow); axial T2 WI (**b**) and ADC (**c**) maps show intermediate T2 signal and low ADC values indicative of low cellularity; axial post-contrast T1 WI (**d**) shows homogeneous tumoural enhancement

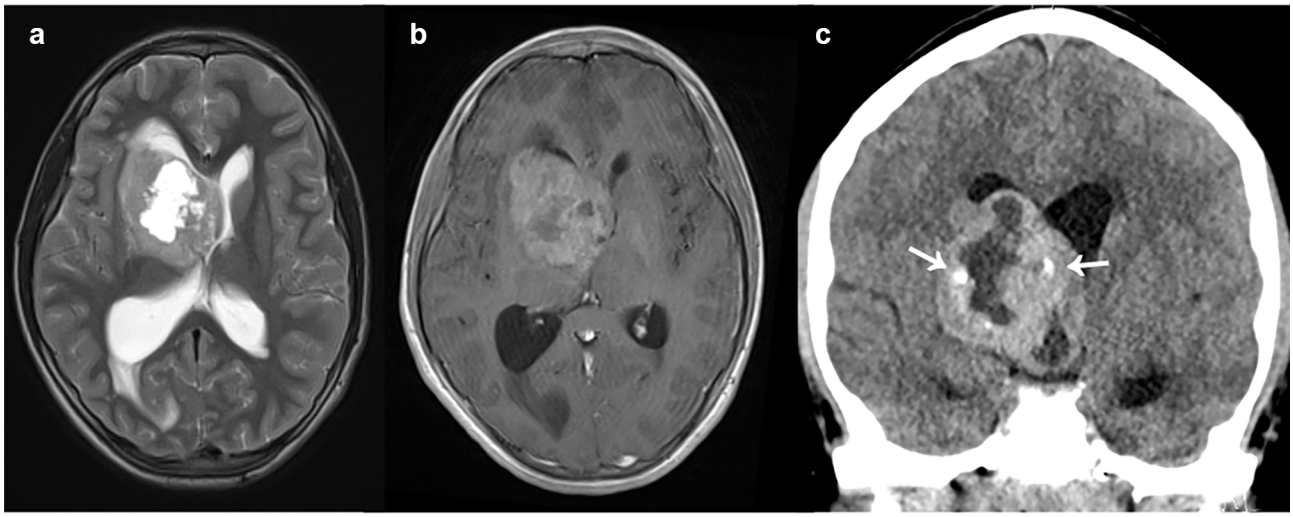

Fig. 2 Axial T2 WI (**a**), axial post-contrast T1 WI (**b**) and coronal unenhanced CT (**c**) show a germinoma with basal ganglia involvement; note the internal calcifications, which are well demonstrated on unenhanced CT (arrows in c)

in differentiation between germinomas and pineoblastomas; whilst the latter is associated with a lower ADC [16], a degree of overlap exists [17] and additional supportive imaging features should be sought to improve diagnostic confidence. Foci of calcification or haemorrhage may be seen on T2* GRE/SWI, and internal cystic structures may be present. Nevertheless, the internal architecture tends to be fairly homogeneous, and any marked heterogeneity (corresponding to haemorrhagic/cystic components or the presence of fat) is more suggestive of a nGGCT [18]. Moderate to strong enhancement following gadolinium administration is typical (Fig. 1d). An absent posterior pituitary bright spot on T1WI is frequently encountered and is associated with the presence of central diabetes insipidus [19].

Primary basal ganglia and thalamic involvement is rare and may have subtle or potentially absent imaging findings in the early stages of disease. In such cases, the lesion is classically periventricular or located within the posterior limb of the internal capsule. Little to no associated mass effect is often observed, although a large space occupying lesion may rarely occur [20, 21] (Fig. 2). Calcified foci on CT (Fig. 2c), hypointensity on T2* GRE/SWI [18] and ipsilateral atrophy of the cerebral hemisphere or cerebral peduncle may act as additional indicators of basal ganglia involvement, contributing to earlier diagnosis and treatment.

The suprasellar region should be evaluated for thickening of the infundibulum or the presence of an additional lesion of similar imaging features, which would be suggestive of a bifocal germinoma (Fig. 3). If additional sites of disease are found, the germinoma is classified as metastatic.

Hydrocephalus may be present, although this finding is most frequently associated with pineoblastoma. Germinomas are non-encapsulated tumours with a propensity for invasion and CSF dissemination. As such, if a pineal germinoma is suspected, the MR of the entire neuraxis should be imaged [22]. MRS may demonstrate elevated lipids and taurine, although these features are not specific and not always present. Following radiotherapy, a reduction in volume and an increase in ADC values has been associated with a positive treatment response [23].

Midline nGGCTs

Non-germinomatous germ cell tumours (nGGCTs) are a rare group of midline, histologically variable neoplasms which occur infrequently in the CNS. This category is inclusive of teratomas, yolk sac tumours, choriocarcinoma, embryonal carcinoma and mixed germ cell tumours. The peak incidence

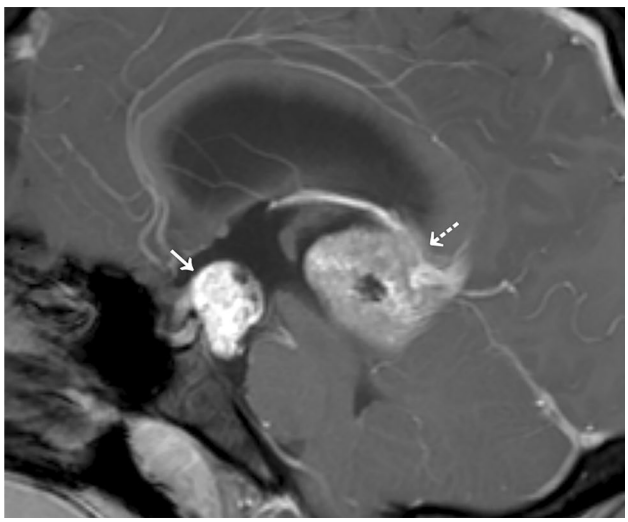

Fig. 3 Sagittal post contrast T1 WI shows a bifocal germinoma in the anterior aspect of the third ventricle (short arrow) and in the pineal region (dotted arrow)

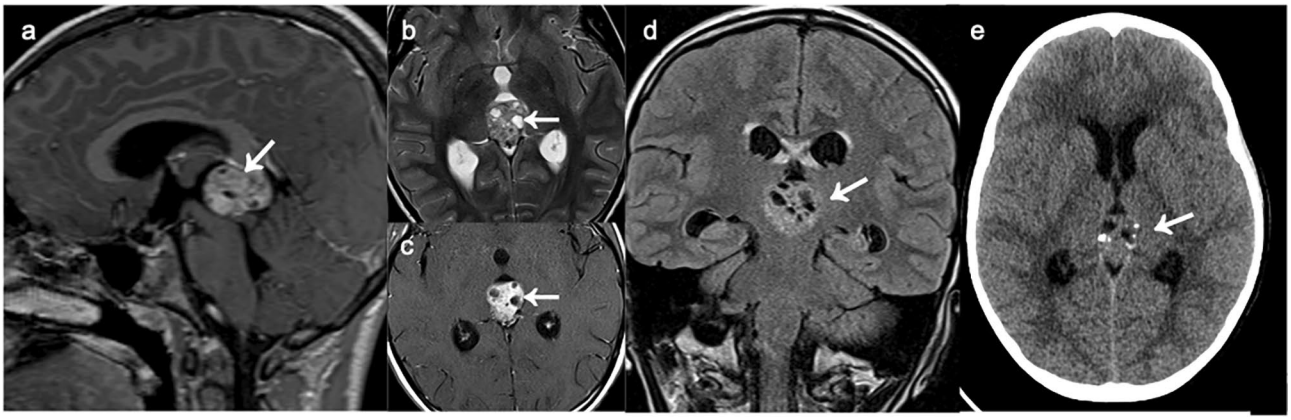

Fig. 4 Sagittal and axial post-contrast T1 WI (**a** and **c**), axial T2 WI (**b**), coronal FLAIR (**d**) and axial unenhanced CT (**e**) in a patient with a nGCCT (arrows); note the internal heterogeneity of the mass (despite its small size), which is more suggestive of nGCCT over germinoma

of nGGCTs occurs in adolescence, slightly earlier than the overall peak incidence for germinoma [9, 24]. nGGCTs confer a poorer prognosis [9], except for mature teratoma.

Other than the mature teratoma discussed below, nGGCTs are associated with non-specific, often aggressive imaging findings which can limit reliable differentiation of nGGCTs from other tumours such as germinoma. nGCCTs are typically located in the pineal region and are frequently more heterogeneous than germinoma (Fig. 4). SWI has been postulated to add further value in this setting [18], as haemorrhage is atypical in midline germinomas, whereas it is frequent in nGGCT. Calcification may be present in both entities. Regions of hypointensity on SWI may predict areas of metastatic disease prior to the development of pathological contrast enhancement [18], thus may have a future role in the follow-up of nGGCT.

In the setting of a suspected nGGCT, tumour markers play an important role in aiding the diagnostic process [7]: (1) elevated βHCG is associated with choriocarcinomas, syncytiotrophoblastic germinomas, and mixed GCT; (2) alpha-fetoprotein (AFP) is increased in yolk sac tumours, immature teratomas and mixed GCT; and (3) raised placental alkaline phosphatase (PLAP) is associated with embryonal carcinomas, yolk sac tumours, choriocarcinomas, syncytiotrophoblastic germinomas and mixed GCT.

Teratoma

Teratomas consist of tissue derived from all three germ cell layers, including sebaceous fat. Teratomas are the second most common nGGCT and may be classified as differentiated/ 'mature', poorly differentiated/ 'immature', or those with malignant transformation [25]. The typical imaging findings of a mature pineal teratoma are that of a lobulated, heterogeneous pineal gland mass comprising a mixture of variable tissue densities/signal intensities including fat (which is the most important element for the diagnosis, corresponding to hypodensity on CT, hyperintensity on T1WI and hypointensity on fat suppression sequences), calcification, cystic and solid components (Fig. 5).

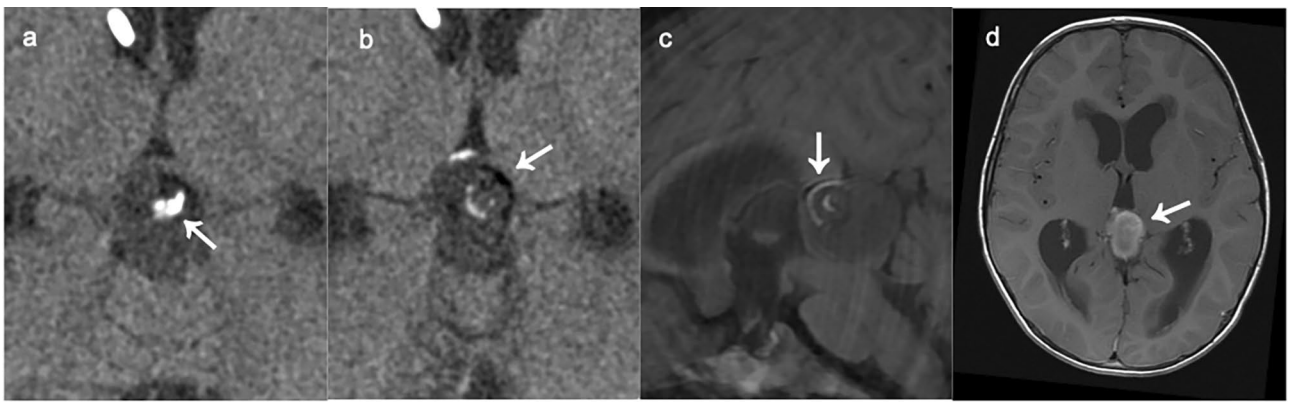

Fig. 5 Pineal teratoma: axial unenhanced CT shows calcification (arrow in **a**) and fatty hypodense components (arrow in **b**). The fat is also hyperintense on T1 WI pre contrast (arrow in **c**), whilst the post-contrast axial T1 WI shows homogeneous enhancement (arrow in **d**). Use of multiparametric imaging to identify different components of the mass is critical for the diagnosis

The differential diagnosis for a midline, inhomogeneous fat containing lesion includes a dermoid cyst [26]. In contradistinction to teratomas, dermoid cysts do not arise from the pineal gland, are less complex, do not have solid enhancing components and are typically asymptomatic unless ruptured. The presence of aggressive features such as local invasion may suggest malignant transformation or an immature subtype. Immature teratomas are usually congenital [27] and confer a poor prognosis [27], with a propensity for early recurrence and metastasis [28]. Imaging features are less specific when compared to mature teratomas; the mass is typically larger, and there may be little to no appreciable fat component.

Pineal parenchymal tumours

Pineal parenchymal tumours are a group of primary pineal tumours that arise directly from pineocytes. They are relatively uncommon, representing approximately 15% of pineal region tumours [15].

Pineoblastoma

Pineoblastoma, a WHO grade IV neoplasm, is the most aggressive entity amongst the pineal tumours with a poor prognosis [29]. Pineoblastomas are rare and occur mostly in infancy and childhood, with a median age at diagnosis of 4.9 years [30]. As a highly cellular embryonal tumour, they share imaging characteristics with other embryonal neoplasms (including medulloblastoma, atypical teratoid rhabdoid tumour, etc.) such as diffusion restriction, which is a key differentiator from low grade tumours. Conversely, contrast enhancement is variable and less useful for the differential diagnosis. Whilst hydrocephalus may occur in any pineal region neoplasm, it is most frequently associated with pineoblastoma. There is a propensity for rapid growth, early invasion of adjacent brain structures and CSF dissemination. Rarely, pineoblastomas can occur in conjunction with retinoblastoma, a configuration termed 'trilateral retinoblastoma'. In such cases, the presence of a germline RB1 pathogenic variant should be investigated (Fig. 6).

On CT, pineoblastomas are large and hyperdense. Calcification is frequent; whilst the distribution is classically described as peripheral or 'exploded' [15] (in contradistinction to the central, 'engulfed' calcification in germinoma), the pattern of calcification in both entities can be variable. Internal haemorrhagic and cystic components may also be seen. MRI features are frequently heterogeneous and variable. A low intrinsic ADC value is a key characteristic feature and related to high cellularity. Reduced ADC values

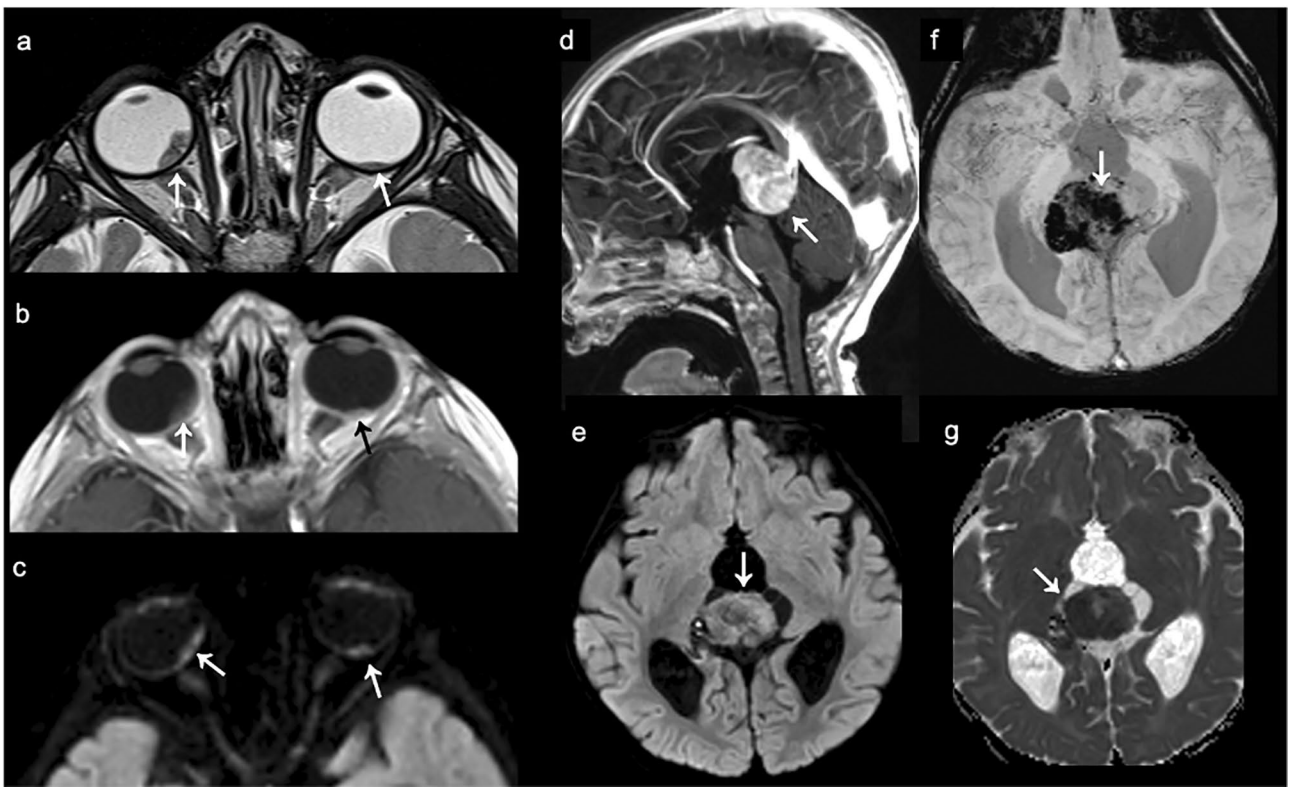

Fig. 6 Trilateral retinoblastoma. Bilateral retinoblastomas are well demonstrated on axial T2 WI (arrows in **a**), axial T1 WI post-contrast (**b**) and DWI (**c**) with enhancement and diffusion restriction evident (arrows in **b** and **c**, respectively). An associated pineoblastoma shows marked enhancement (arrow in **d**), diffusion restriction on DWI and ADC maps (arrow in **e** and **g**) and internal calcification on SWI (arrow in **f**)

are also a prominent finding in germinoma [16] or pineal parenchymal tumours of intermediate differentiation; whilst these entities may be challenging to differentiate by imaging criteria alone, the demographics of the patient is critical, as the age of peak incidence in pineoblastoma is significantly lower. Enhancement characteristics are extremely variable. T2* GRE/SWI may demonstrate foci of hypointensity related to calcification and/or haemorrhage. A variable degree of perilesional vasogenic oedema in the surrounding parenchyma can be present, and invasion of adjacent structures may be evident on T2W/post-contrast imaging. CSF dissemination is frequent and the entire neuroaxis should be imaged, as for other tumours in this region. Synchronous suprasellar and pineal involvement favours a bifocal germinoma, whereas involvement of the globes should raise the possibility of a trilateral retinoblastoma. MRS may demonstrate a non-specific increase in choline and decreased NAA. An increased lipid and taurine peak may also be noted, similar to germinoma [31]. An important association with the *SMARCB1* mutation and synchronous rhabdoid tumours in the soft tissues has been described [16].

Pineal parenchymal tumours of intermediate differentiation

Pineal parenchymal tumours of intermediate differentiation (PPTID) are WHO grade II–III tumours which share overlapping imaging features with pineoblastomas and pineocytomas [32]. Neuroimaging characteristics are variable but typically that of a moderately aggressive neoplasm of variable size and intermediary imaging features [32], including reduced ADC values in some cases. Rarely, aggressive findings may be present. Whilst PPTID can occur at any age, they are often encountered in middle-aged adults [29], which is useful for the differential diagnosis.

Pineocytoma

Pineocytomas are a relatively indolent, slow growing WHO grade I tumour of the pineal gland, which may occur at any age but are most frequently observed in middle-aged adults [29]. Whilst often an incidental finding, symptomatic cases do occur and are typically related to mass effect on adjacent structures. The typical MR imaging features of a pineocytoma reflect the low grade: a homogeneous, well-circumscribed pineal mass without evidence of restricted diffusion, increased perfusion or local invasion. Homogeneous enhancement, peripheral calcification and cystic or haemorrhagic foci are not infrequent. Rarely, a pineocytoma may be predominantly cystic and mimic a pineal cyst, although a truly simple cyst morphology in this setting is unlikely [33]. CSF dissemination is rare, and recurrence after total resection is undocumented.

Pineal cyst

Pineal cysts are common, typically asymptomatic lesions which are most frequently discovered in young adulthood as an incidental finding. The documented prevalence is up to 20–40% in autopsy series [34]. Rarely, they can be symptomatic due to mass effect on local structures. On imaging, a thin walled, fluid density cyst or multicystic structure is demonstrated [35] (Fig. 7). Aside from rare instances of intracystic haemorrhage, the fluid contents typically mirror CSF on T1/T2WI, but are often hyperintense on FLAIR. Whilst typically subcentimetric, cyst diameters of up to 4 cm have been reported. Calcification and smooth, linear enhancement of the cyst wall are common. When large, pineal cysts may prove a diagnostic dilemma owing to overlapping imaging findings with the rare cystic pineocytoma. Complex features, soft tissue nodularity or atypical enhancement characteristics should raise concern for an alternative diagnosis. Asymptomatic pineal cysts of less

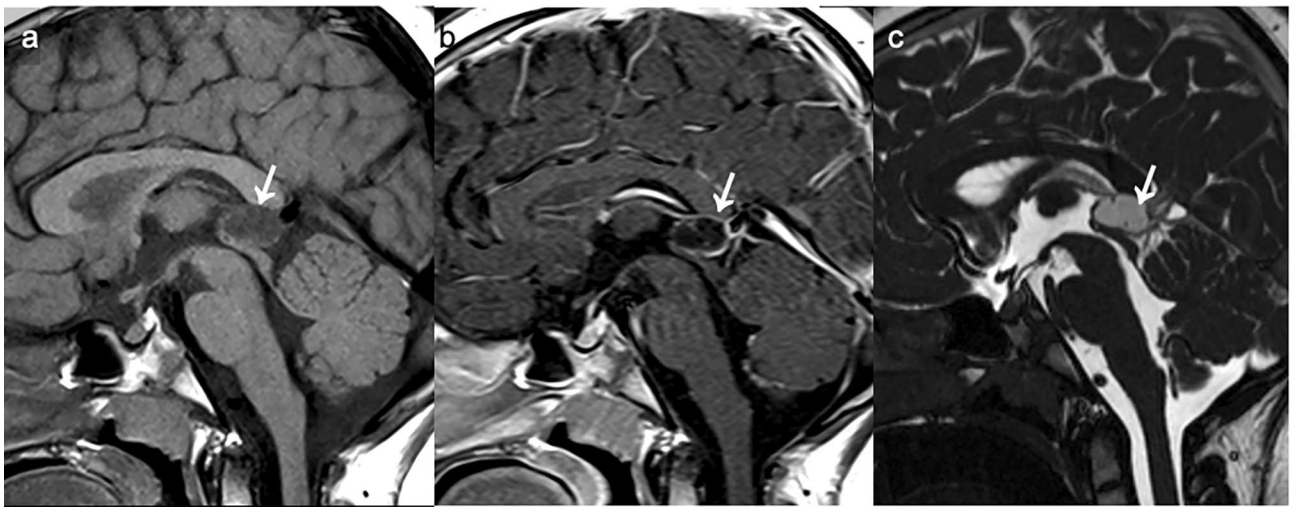

Fig. 7 Sagittal T1 WI pre- (**a**) and post-contrast (**b**) and sagittal CISS (**c**) of a simple pineal cyst (arrows)

Fig. 8 Large craniopharyngioma showing calcification on unenhanced CT (arrow in **a**) and large internal cysts with a small solid component (arrow in **b**). The cyst exhibits intermediate to high signal on T1 WI pre-contrast (arrow in **c**) associated with craniopharyngiomas, and demonstrates peripheral enhancement (arrows in **d**)

than 1 cm with classical imaging appearances do not require follow-up. The serial imaging follow-up of larger cysts remains controversial, given the low incidence of pineal neoplasm and studies documenting stability of such cysts over time [34, 36].

Sellar and suprasellar masses

A variety of solid and cystic lesions can occur in the sellar and suprasellar regions, with frequent overlapping imaging features. Accurate anatomical localization of the tumour is of critical importance, as is the pattern of involvement. A thoughtful search for additional radiological clues, both intracranial and extracranial, can help to refine the differential diagnosis.

Sellar

Craniopharyngioma

Craniopharyngiomas (CPs) are WHO grade I neoplasms. The two major pathological subtypes of craniopharyngioma vary in age of peak incidence, anatomical location, histopathological features and imaging characteristics. CPs classically present in a bimodal distribution, although can occur at any age. The first peak incidence falls between 5 and 14 years of age [37] and corresponds almost entirely to the adamantinomatous subtype (aCP). The squamous papillary subtype is rare in children. Whilst classically suprasellar in location, primary CPs may rarely occur elsewhere, such as the posterior fossa including the cerebellopontine angle [38]. Clinical presentation is variable and includes headache, visual disturbance, hypopituitarism, obesity, diabetes insipidus and other manifestations of endocrine dysfunction. Although histologically benign, CPs are locally aggressive and recurrence and progression are frequent [39].

The typical imaging appearances of CP in children are that of a lobulated, mixed solid/cystic mass in the sellar/suprasellar region, with internal calcification and enhancement [40] (Fig. 8). A normal pituitary gland is frequently seen as a discrete structure. 'The rule of 90' in adamantinomatous CPs refers to the approximate incidence (90%) of calcification, enhancement of solid components and a mixed solid/cystic architecture, which may aid the diagnostic process. On MRI, aCPs can exhibit T1 hyperintense cystic components in 1/3rd of cases, related to proteinaceous contents or methemoglobin. A Rathke cleft cyst (RCC) may also display T1 hyperintensity but is typically smaller, located between the anterior and posterior pituitary gland and lacks solid enhancing components (Fig. 9). A haemorrhagic pituitary adenoma may also

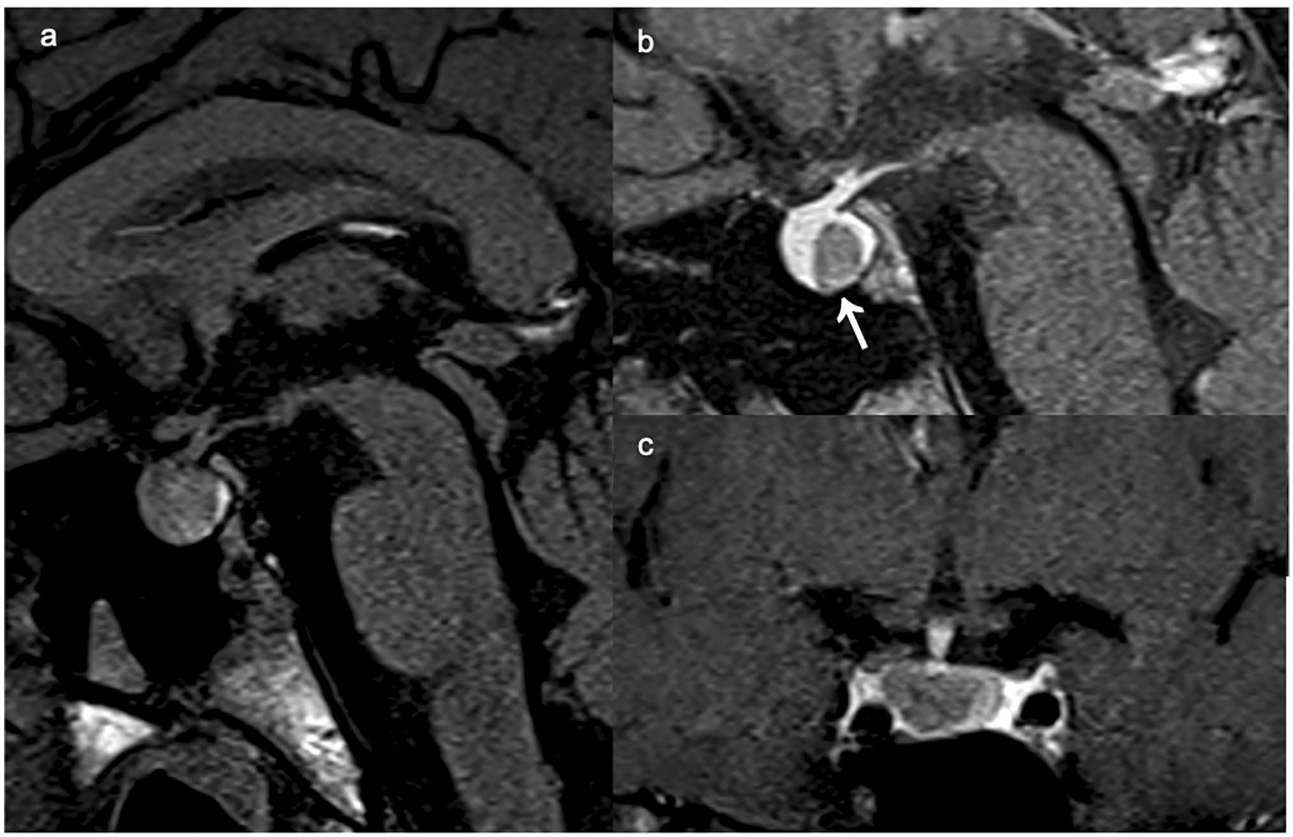

Fig. 9 Rathke cleft cyst on sagittal T1 WI pre-contrast (**a**), sagittal (**b**) and coronal (**c**) post-contrast images. Note the relative hypointensity of the cyst in comparison to the remaining enhancing glandular parenchyma (arrow in **b**)

demonstrate T1 shortening, although is generally T2 hypointense secondary to deoxyhemoglobin. Lesion characteristics on T2WI are variable, depending on the proportion of cystic and solid components. DWI characteristics also vary and are partially attributable to the density of fluid constituents. Avid contrast enhancement of the solid components and cyst walls is typical. Hypointensity on T2* GRE/SWI corresponds to regions of haemorrhage and calcification. In contradistinction, calcification is rare in pituitary macroadenomas, representing another element useful for the differential diagnosis. MRS may demonstrate a broad lipid peak, corresponding to the cholesterol content within the tumoural cysts. The squamous papillary subtype of CP is predominantly solid; cystic components are usually less prominent and similar in signal intensity to CSF. Presentation in childhood, T1 hyperintensity and calcification on CT favour aCP [40]. However, it should be noted that there is a degree of overlap in the radiological features of CP subtypes. In the suprasellar compartment, hypothalamic and optic pathway gliomas should remain a consideration, although the anatomical origin is distinct, enhancement is typically less marked and a prominent cystic component or calcification would be unusual.

Pituitary adenoma

Pituitary adenomas comprise approximately 2.7% of supratentorial tumours in children [41] and rarely present before puberty [42]. Adenomas are classified as microadenomas or macroadenomas based on a maximum diameter of less than, or greater than 10 mm, respectively. In children, microadenomas predominate [43] and non-functioning pituitary adenomas are rare [44]. Clinical presentation is typically related to a hypersecretory syndrome, such as growth retardation or primary amenorrhoea, although large macroadenomas may occasionally present with symptoms of mass effect, including headache, visual symptoms or hydrocephalus. Rarely, a pituitary adenoma may exist in the context of a genetic syndrome, such as multiple endocrine neoplasia (I or IV), Carney complex, McCune Albright syndrome or familial isolated pituitary adenoma [44].

On standard MRI sequences, small microadenomas may be difficult to visualise or may be indistinguishable from a Rathke cleft/pars intermedia cyst. On thin section coronal dynamic contrast-enhanced imaging, microadenomas typically appear hypointense relative to the rapidly enhancing pituitary gland during early image acquisition, progressing to isointensity at later time points. Physiological pituitary hyperplasia is an important consideration in such cases, particularly during puberty. In the presence of a diffusely enlarged pituitary gland without a visible causative lesion on MRI, correlation with pituitary function studies is important to avoid over/misdiagnosis.

Conversely, the typical imaging features of a macroadenoma are that of a sellar/suprasellar mass which fills/expands the sella turcica and is inseparable from the pituitary gland (Fig. 10). In the event of suprasellar extension,

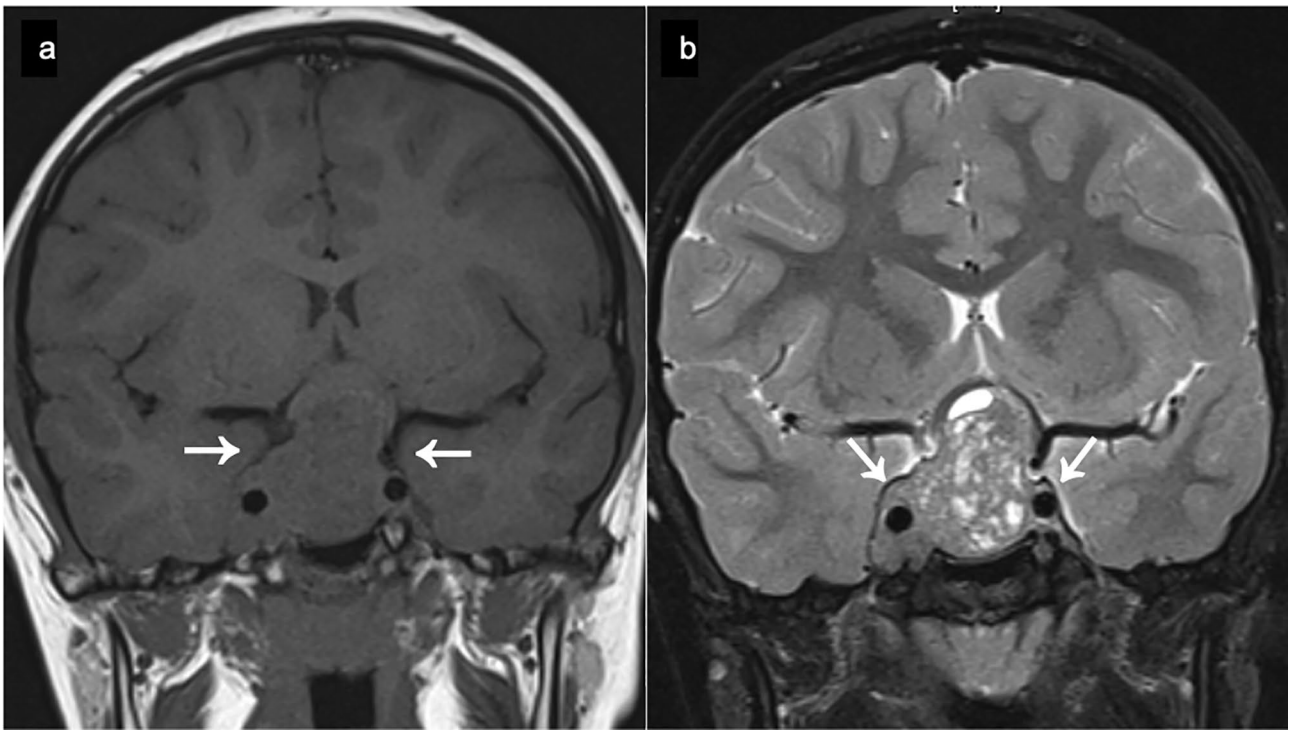

Fig. 10 Typical appearance of a pituitary macroadenoma on coronal pre contrast T1 WI (**a**) and coronal T2 WI (**b**). Note the 'snowman'/ '8' morphology and the invasion of the cavernous sinus (arrows)

a 'snowman'/ '8' morphology is often noted due to impedance from the diaphragm sellae. The pituitary bright spot is generally displaced superiorly or absent. An enhancing dural tail is infrequently present and may mimic a meningioma, although paediatric meningiomas are unusual in the absence of neurofibromatosis type 2 and should be identifiable as a distinct structure from the pituitary gland. Small cystic and haemorrhagic foci are relatively frequent, but calcification is rare, in contradistinction to craniopharyngioma. Fluid–fluid levels and major haemorrhagic transformation are possible, but are more typical in the context of pituitary apoplexy. Extension into the cavernous sinuses is common; the degree of encasement of the internal carotid arteries can predict sinus invasion and is important in pre-operative planning [45, 46]. Similarly, the relationship to, and any compression of the suprasellar and parasellar structures including the optic chiasm and midbrain should be assessed.

Infundibular

The normal pituitary stalk (infundibulum) tapers smoothly as it descends towards the pituitary gland, measuring approximately 3.25 ± 0.56 mm in diameter at the level of the optic chiasm, and 1.91 ± 0.40 mm at its insertion into the pituitary gland [47]. In addition to the neoplastic causes discussed in this article, infundibular pathology may also be infectious, inflammatory or developmental in aetiology, which should remain a consideration.

Langerhans cell histiocytosis

Langerhans cell histiocytosis (LCH) is a systemic disorder characterised by the proliferation and accumulation of Langerhans cells. CNS involvement is rare in isolation and typically occurs in conjunction with extracranial manifestations. The key features of CNS LCH are hypothalamic–pituitary axis (HPA) involvement, bony involvement and neurodegeneration [48]. The most common endocrine manifestation of LCH is diabetes insipidus.

Skull X-ray, CT with bone reconstructions or brain MRI may demonstrate solitary or multifocal, well-circumscribed lytic lesions within the skull (Fig. 11a). In the calvarium, the parietal bone is most frequently involved, whereas the temporal bone is the most commonly affected within the skull base [48]. The lesions frequently demonstrate a beveled edge, secondary to asymmetrical involvement of

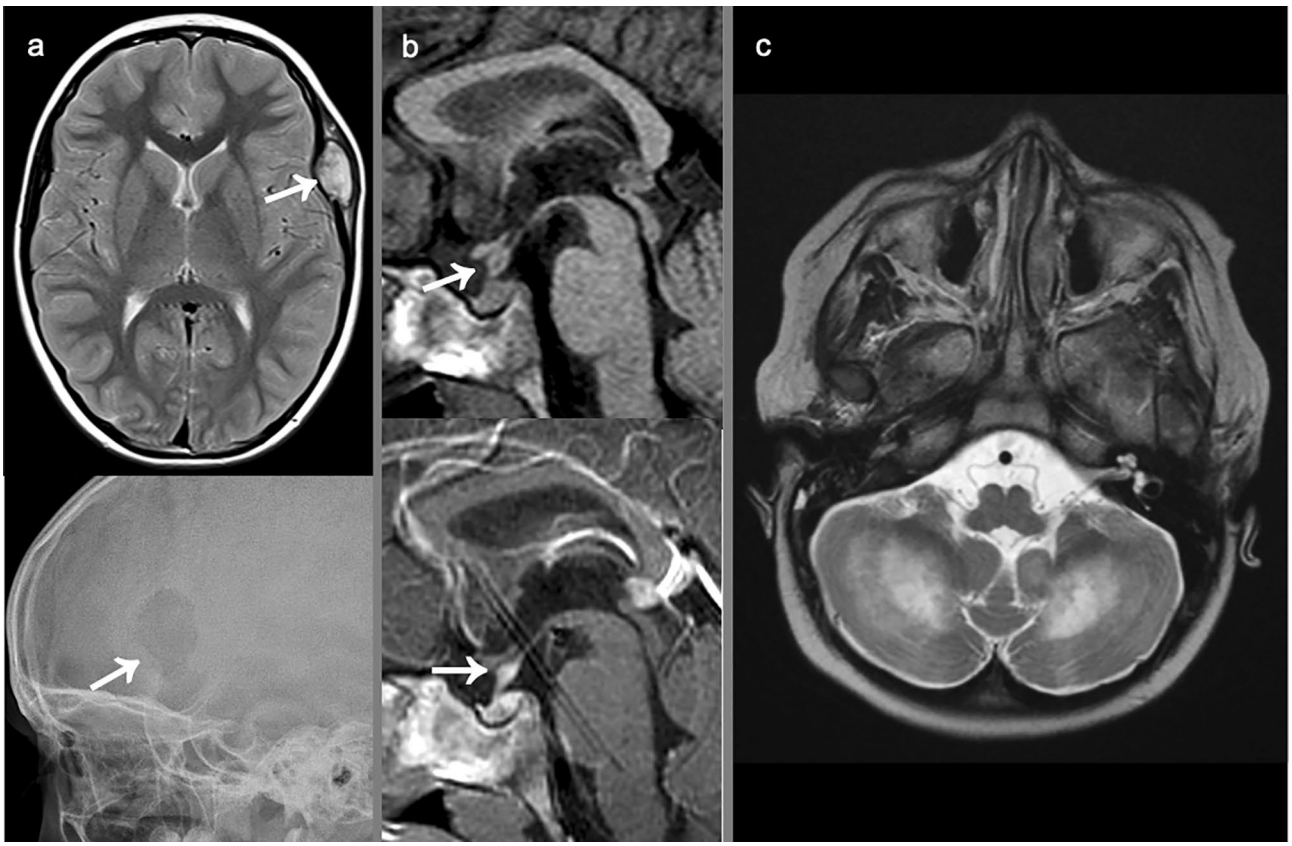

Fig. 11 Langerhans cell histiocytosis: axial T2 WI and skull radiograph (**a**) show a lytic lesion in the skull (arrows). Thickening of the stalk is evident on T1 WI pre- and post-contrast (arrows in **b**). Axial T2 WI of the brain shows typical signal changes within the cerebellar hemispheres (**c**)

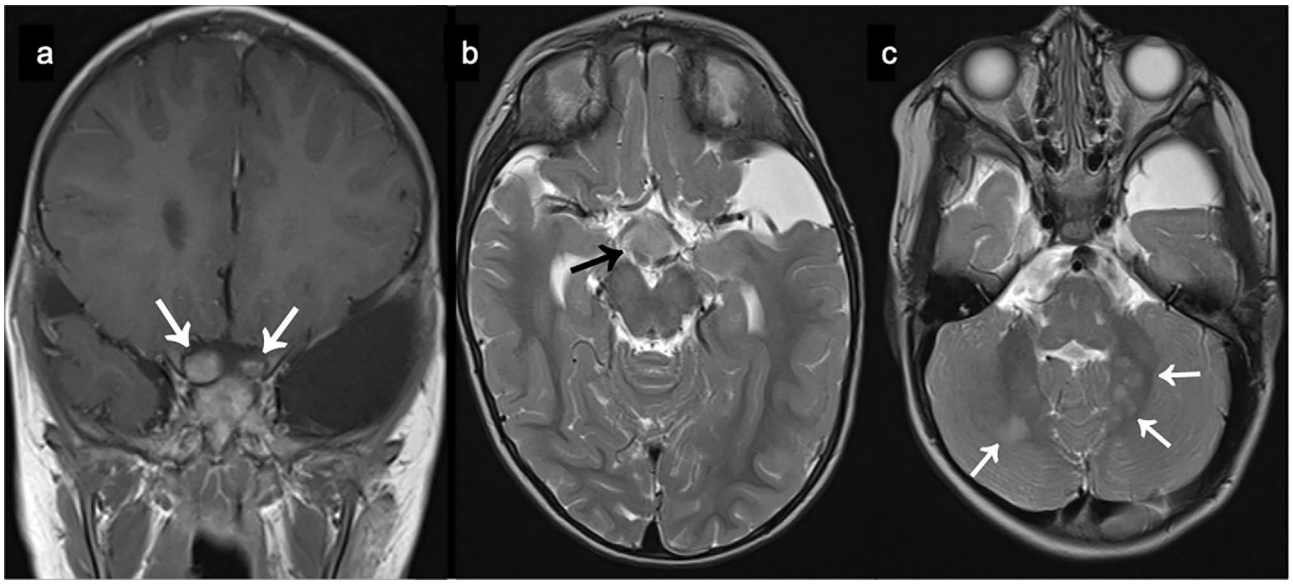

Fig. 12 Coronal T1 WI post-contrast (**a**), axial T2 WI (**b**) show an optic pathway glioma involving the optic nerves (arrows in **a**) and the chiasm (arrow in **b**). Axial T2 WI at the level of the cerebellum (**c**) shows typical NF1 related foci of abnormal signal intensity (FASI) (arrows)

the inner and outer table. An associated soft tissue mass may be present, with homogeneous contrast enhancement on CT/MRI but without marked diffusion restriction on DWI (which is useful in the differential diagnosis with skull metastases from a neuroblastoma). The most characteristic imaging finding on MRI is thickening of the infundibulum (Fig. 11b) to a diameter greater than 3 mm and an absent posterior pituitary bright spot on T1WI (high-resolution 3D sequences such as CISS, FIESTA and DRIVE are useful for infundibular measurements). The HPA features in LCH

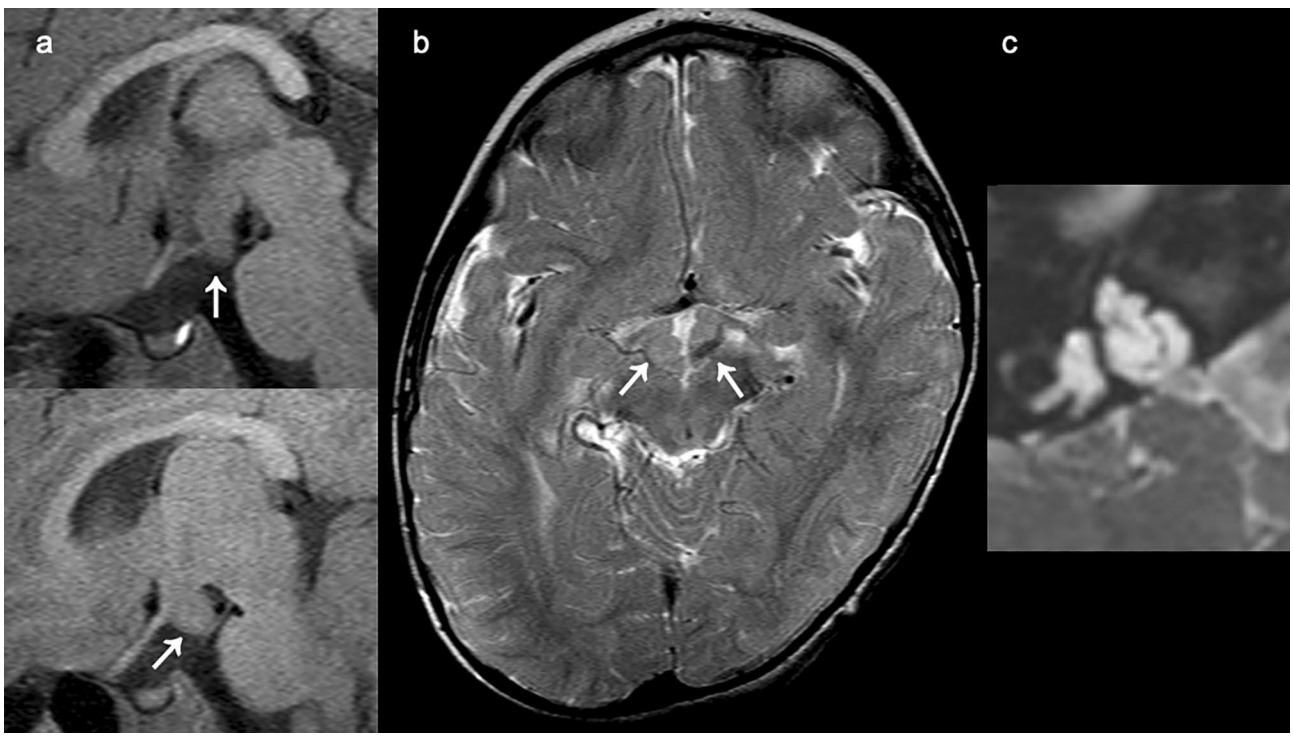

Fig. 13 Patient with X-linked deafness due to *POU3F4* mutation. There is a hypothalamic malformation resembling a hamartoma, demonstrated on sagittal T1 WI (arrows in **a**). Axial T2 WI shows a bulky appearance of the hypothalamus (arrows in **b**). Note the typical incomplete partition type 3 malformation of the cochlea in these patients (**c**)

Table 3 Main radiological findings of pineal, sellar and suprasellar tumours

Pineal tumour	Second/associated location	Peak age	CT	MRI (T1)	MRI (T2)	MRI (CE)	MRI (ADC)[a]	MRI (SWI)	Ca^{2+}	Haem	CSF dissemination	Other
Germinoma	Pineal +/− suprasellar (rarely BG, thalamus, cerebellum, SC)	Adolescence	Hyperdense	Iso	Hypo to iso +/− small internal cysts	Homogeneous	↓	+	+(+/− engulfed)	+/−	++	Male predominance Bifocal lesions common (infundibular stalk, anterior third ventricular recesses Absent posterior pituitary bright spot suggestive of associated DI
Midline nGGCT	Pineal	Adolescence (slightly earlier than germinoma)	Heterogeneous	Variable	Variable, heterogeneous	Heterogeneous	Variable	+(Ca, haem, iron)	+	++	+	Imaging features often non-specific and aggressive; correlation with tumour markers may be helpful
Mature teratoma	Pineal	Mid adolescence	Heterogeneous +/− fat density components	Mixed +/− hyper	Variable	Heterogeneous, variable	=	+	+	+	+/−	
Immature teratoma	Pineal	Foetus/Newborn	Heterogeneous, large	Variable	Variable	Variable	Variable	++	++	++		Large, aggressive mass Poor prognosis
Pineoblastoma	-	5 years	Hyperdense, heterogenous	Hypo to iso	Hypo/iso +/− hyperintense cystic components	Variable	↓	+	+(+/− exploded)	+/−	++	Obstructive hydrocephalus and local invasion common Can occur in context of retinoblastoma
PPTID	-	Adolescence to adulthood	Variable	Iso	Iso to hyper	Heterogeneous	=/↓	+/−	+/−	+/−	+(rare)	
Pineocytoma	-	Adulthood	Hypo to isodense	Iso to hypo	Iso to hyper	Homogeneous, heterogeneous or peripheral	=	+	+(+/− exploded)	+/−	-	Well circumscribed Cysts are common. Rarely, predominantly cystic and may mimic a pineal cyst
Pineal cyst	-	Young adulthood	Hypodense, uni or multilocular	Hypo	Hyper	+/− linear peripheral enhancement	↑	+/−	+	-	-	Cyst contents often hyperintense on FLAIR

Table 3 (continued)

Sellar/suprasellar tumour	Location	Peak age	CT	MRI (T1)	MRI (T2)	MRI (CE)	MRI (ADC)[a]	MRI (SWI)	Ca^{2+}	Haem	CSF dissemination	Other
Craniopharyngioma (adamantinomatous)	Sellar/suprasellar	5–14	Mixed solid/cystic	Mixed +/− hyper	Variable	Heterogeneous (cyst walls + solid components)	Variable	++	++	-	-	Locally aggressive, high local recurrence rate +/− hyperintensity along optic tracts usually related to oedema
Craniopharyngioma (papillary)	Sellar/suprasellar	Middle-aged adulthood	Predominantly solid	Hypo to iso	Variable	Present, variable	Variable	+/−	+/− (rare)	+/−	-	Rare in children, but overlapping imaging findings with aCP
Rathke cleft cyst	Sellar (between anterior lobe and pars intermedia) or suprasellar	Any	Hypodense > hyperdense	Hypo to hyper	Hyper > iso/hypo	None +/− claw of peripheral enhancing pituitary tissue	↑	− (unless haemorrhagic)	-	+/− (may haemorrhage)	-	+/− non-enhancing intracystic nodule FLAIR hyperintense Usually incidental but can be symptomatic when large
Pituitary macroadenoma	Sellar +/− suprasellar	Puberty	Isodense but variable	Iso	Iso > variable	Heterogeneous	=/↑	+/− (if haemorrhagic)	− (rare)	+/− (if haemorrhagic)	-	Dural tail in 5–10% of cases +/− enlarged sella turcica, absent pituitary bright spot, cavernous sinus invasion
Pituitary microadenoma	Sellar	Puberty	Isodense	Iso	Hypo to hyper	Reduced and delayed enhancement relative to normal pituitary tissue	=	+/−	− (rare)	+/−	-	
Langerhan cell histiocytosis	Infundibular	Childhood	Thickened pituitary stalk	Iso	Iso to hyper	Avid, homogeneous	=	-	-	-	- (leptomeningeal abnormalities may occur as a distinct process)	Non-specific—look for additional sequelae e.g. lytic skull lesions with bevelled edges. Absence of the pituitary bright spot

Table 3 (continued)

Sellar/suprasellar tumour	Location	Peak age	CT	MRI (T1)	MRI (T2)	MRI (CE)	MRI (ADC)[a]	MRI (SWI)	Ca^{2+}	Haem	CSF dissemination	Other
Hypothalamic/optic pathway glioma	Suprasellar, optic pathway or hypothalamus	Childhood	Hypodense, solid	Iso to mild hypo	Hyper	Sporadic: Moderate to strong NF1: Variable/ absent	↑	±	+/−(rare)	-	-	Fusiform enlargement of optic chiasm and/ or hypothalamus Majority WHO G1 PA Association with NF1
Hypothalamic hamartoma	Tuber cinereum	Infancy	Iso to slightly hypodense	Iso to slightly hypo	Iso to slightly hyper	None	=	-	-	-	-	Typical clinical presentation Sessile (gelastic epilepsy) or pedunculated (precocious puberty). Can be observed in the context of ciliopathies (Joubert syndrome) and midline defects
Interhypothalamic adhesion	Anteroinferior third ventricle, connecting hypothalami	Infancy	Isodense	Iso	Iso	None	=	-	-	-	-	Typical location/ morphology Strong association with structural brain abnormalities such as Chiari II

nGGCT non-germinomatous germ cell tumour, *PPTID* pineal parenchymal tumour of intermediate differentiation, *Ca^{2+}* calcification, *Haem* haemorrhage, *CSF* cerebrospinal fluid, *BG* basal ganglia, *SC* spinal cord, *DI* diabetes insipidus, *PA* pilocytic astrocytoma, *NF1* neurofibromatosis type 1

[a]Important to analyse this feature in solid areas without calcium or haemorrhage

are non-specific and overlap with lymphocytic hypophysitis, germinomas and neurosarcoidosis; correlation with associated imaging features can aid differentiation. Parenchymal findings on T2WI include enlarged perivascular spaces, bilateral symmetric lesions of variable signal intensity within the cerebellum (including the dentate nuclei) and basal ganglia, and cerebral atrophy (Fig. 11c). Rarely, focal masses arising from the meninges, choroid plexus or basal ganglia may occur.

Suprasellar

Hypothalamic and chiasmatic optic pathway glioma

Optic pathway gliomas (OPGs) are rare astrocytic tumours which account for 3–5% of intracranial paediatric tumours. In the paediatric population, they are often low grade and associated with neurofibromatosis type 1 (NF1). The majority are WHO grade I pilocytic astrocytomas (PAs); the remainder are pilomyxoid astrocytomas (PMAs) which are associated with a younger age of onset and a higher rate of recurrence and CSF dissemination [49]. Whilst paediatric OPGs are rarely fatal and may be clinically indolent, they can also be associated with significant morbidity, such as visual impairment, raised intracranial pressure and hypothalamic dysfunction.

Imaging appearances on CT include enlargement of the optic chiasm or hypothalamus (Fig. 12). MRI may demonstrate fusiform enlargement and hyperintensity of the chiasm and/or hypothalamus on T2WI/FLAIR, with iso- to mild hypointensity on T1WI. Intratumoural haemorrhage with resultant T1 hyperintensity is associated with the more aggressive PMA subtype, and the adjacent parenchyma and subarachnoid spaces should be assessed for evidence of invasion or dissemination, respectively. Contrast enhancement is typically present and heterogeneous, often with an 'out-of-focus' pattern. The enhancement pattern may vary throughout the clinical course (disappearing with some chemotherapy), and an increase in enhancement without a concurrent increase in size should not be considered progression [50]. OPGs do not exhibit restricted diffusion on DWI, owing to their low cellularity. The Dodge classification, or modifications thereof [51], are based on anatomical localization (presence of optic nerve involvement alone, chiasmal involvement with or without optic nerve involvement and hypothalamic/parasellar involvement) and used to assist patient selection for surgery. In the setting of NF1, the brain should be interrogated for associated radiological features, including ill-defined areas of T2/FLAIR hyperintensity (FASI) (Fig. 12c), sphenoid wing hypoplasia, plexiform neurofibromas and NF1-related moya moya.

Hypothalamic hamartoma

Hypothalamic (tuber cinereum) hamartomas (HH) are a benign, non-neoplastic hamartoma arising from the tuber cinereum, a hypothalamic structure located between the mamillary bodies and optic chiasm. HHs are classically associated with precocious puberty, gelastic seizures, and developmental delay. Symptoms frequently begin in early infancy and result in progressive disability. Onset during adulthood is associated with non-gelastic seizures and a milder clinical course.

On CT or MRI, a sessile or pedunculated mass in the expected location of the tuber cinereum is seen. The lesion is typically similar to grey matter on all sequences (with T2 hyperintensity in some cases), and does not enhance [52]. Reference should be made to the size of the lesion, plane of insertion on the hypothalamus and the presence of intraventricular extension, which form the basis of the Delalande anatomical classification that can influence pre-operative planning [53].

The differential diagnosis of HH is limited due to its characteristic imaging profile. Other local considerations include an interhypothalamic adhesion (IHA), a horizontal band of parenchyma connecting the hypothalami across the antero-inferior third ventricle [54]. Of note, hypothalamic hamartomas are associated with inner ear dysplasias in Pallister-Hall syndrome and X-linked deafness (Fig. 13). As such, the ears and temporal bone structures should be reviewed [55].

Table 3 summarises the main radiological findings of pineal, sellar and suprasellar tumours.

Conclusion

Pineal, sellar and suprasellar tumours in children include an expansive range of entities with a range of overlapping imaging findings. Neuroimaging plays a key role in the diagnosis and management and follow up of these patients. Familiarity with these appearances is vital in improving patient outcomes. Correlation with clinical information including the age of the patient, diffusion status, SWI findings and tumour markers can provide useful additional information to help to refine the differential diagnosis and provide an optimum standard of care.

Author contribution All authors contributed to the conception and design of the article. Initial literature search and material preparation was performed by Emma Lim, Cesar Alves, Stefania Picariello, and Felice D'Arco. The first draft of the manuscript was written and revised by Emma Lim, Cesar Alves, and Felice D'Arco, and all authors commented on subsequent versions of the manuscript. All authors read and approved the final manuscript.

Availability of data and material Data sharing not applicable to this article as no datasets were generated or analysed during the current study.

Declarations

Conflict of interest The authors declare no competing interests.

References

1. Desandes E, Guissou S, Chastagner P, Lacour B (2014) Incidence and survival of children with central nervous system primitive tumors in the French National Registry of Childhood Solid Tumors. Neuro Oncol 16:975–983. https://doi.org/10.1093/neuonc/not309
2. Mottolese C, Szathmari A, Beuriat PA (2015) Incidence of pineal tumours. A review of the literature. Neurochirurgie 61:65–69. https://doi.org/10.1016/j.neuchi.2014.01.005
3. Hoffman HJ, Yoshida M, Becker LE, Hendrick EB, Humphreys RP (1994) Pineal region tumors in childhood. Experience at the Hospital for Sick Children. 1983. Pediatr Neurosurg 21:91–103; discussion 104. https://doi.org/10.1159/000120821
4. Hoffman HJ, Yoshida M, Becker LE, Hendrick EB, Humphreys RP (1984) Experience with pineal region tumours in childhood. Neurol Res 6:107–112. https://doi.org/10.1080/01616412.1984.11739672
5. Allen JC (1987) Management of primary intracranial germ cell tumors of childhood. Pediatr Neurosci 13:152–157. https://doi.org/10.1159/000120321
6. Hoffman HJ, Otsubo H, Hendrick EB, Humphreys RP, Drake JM, Becker LE, Greenberg M, Jenkin D (1991) Intracranial germ-cell tumors in children. J Neurosurg 74:545–551. https://doi.org/10.3171/jns.1991.74.4.0545
7. Echevarría ME, Fangusaro J, Goldman S (2008) Pediatric central nervous system germ cell tumors: a review. Oncologist 13:690–699. https://doi.org/10.1634/theoncologist.2008-0037
8. Wang Y, Zou L, Gao B (2010) Intracranial germinoma: clinical and MRI findings in 56 patients. Childs Nerv Syst 26:1773–1777. https://doi.org/10.1007/s00381-010-1247-2
9. Jennings MT, Gelman R, Hochberg F (1985) Intracranial germ-cell tumors: natural history and pathogenesis. J Neurosurg 63:155–167. https://doi.org/10.3171/jns.1985.63.2.0155
10. Cuccia V, Galarza M (2006) Pure pineal germinomas: analysis of gender incidence. Acta Neurochir (Wien) 148: 865–871; discussion 871. https://doi.org/10.1007/s00701-006-0846-x
11. Sano K (1983) Pineal region tumors: problems in pathology and treatment. Clin Neurosurg 30:59–91. https://doi.org/10.1093/neurosurgery/30.cn_suppl_1.59
12. Phi JH, Wang KC, Kim SK (2018) Intracranial germ cell tumor in the molecular era. J Korean Neurosurg Soc 61:333–342. https://doi.org/10.3340/jkns.2018.0056
13. Minami N, Tanaka K, Kimura H, Hirose T, Mori T, Maeyama M, Sekiya H, Uenaka T, Nakamizo S, Nagashima H, Mizukawa K, Itoh T, Sasayama T, Kohmura E (2016) Radiographic occult cerebellar germinoma presenting with progressive ataxia and cranial nerve palsy. BMC Neurol 16:4. https://doi.org/10.1186/s12883-015-0516-9
14. Loya JJ, Jung H, Temmins C, Cho N, Singh H (2013) Primary spinal germ cell tumors: a case analysis and review of treatment paradigms. Case Rep Med 2013:798358. https://doi.org/10.1155/2013/798358
15. Smirniotopoulos JG, Rushing EJ, Mena H (1992) Pineal region masses: differential diagnosis. Radiographics 12:577–596. https://doi.org/10.1148/radiographics.12.3.1609147
16. Dumrongpisutikul N, Intrapiromkul J, Yousem DM (2012) Distinguishing between germinomas and pineal cell tumors on MR imaging. AJNR Am J Neuroradiol 33:550–555. https://doi.org/10.3174/ajnr.A2806
17. Choudhri AF, Whitehead MT, Siddiqui A, Klimo P Jr, Boop FA (2015) Diffusion characteristics of pediatric pineal tumors. Neuroradiol J 28:209–216. https://doi.org/10.1177/1971400915581741
18. Morana G, Alves CA, Tortora D, Finlay JL, Severino M, Nozza P, Ravegnani M, Pavanello M, Milanaccio C, Maghnie M, Rossi A, Garrè ML (2018) T2*-based MR imaging (gradient echo or susceptibility-weighted imaging) in midline and off-midline intracranial germ cell tumors: a pilot study. Neuroradiology 60:89–99. https://doi.org/10.1007/s00234-017-1947-3
19. Kilday JP, Laughlin S, Urbach S, Bouffet E, Bartels U (2015) Diabetes insipidus in pediatric germinomas of the suprasellar region: characteristic features and significance of the pituitary bright spot. J Neurooncol 121:167–175. https://doi.org/10.1007/s11060-014-1619-7
20. Rasalkar DD, Chu WC, Cheng FW, Paunipagar BK, Shing MK, Li CK (2010) Atypical location of germinoma in basal ganglia in adolescents: radiological features and treatment outcomes. Br J Radiol 83:261–267. https://doi.org/10.1259/bjr/25001856
21. Wei XH, Shen HC, Tang SX, Gao CH, Ren JL, Ai L, Dai JP (2016) Radiologic features of primary intracranial ectopic germinomas: Case reports and literature review. Medicine (Baltimore) 95:e5543. https://doi.org/10.1097/md.0000000000005543
22. Buch K, Caruso P, Ebb D, Rincon S (2018) Balanced steady-state free precession sequence (CISS/FIESTA/3D driven equilibrium radiofrequency reset pulse) increases the diagnostic yield for spinal drop metastases in children with brain tumors. AJNR Am J Neuroradiol 39:1355–1361. https://doi.org/10.3174/ajnr.A5645
23. Ogiwara H, Tsutsumi Y, Matsuoka K, Kiyotani C, Terashima K, Morota N (2015) Apparent diffusion coefficient of intracranial germ cell tumors. J Neurooncol 121:565–571. https://doi.org/10.1007/s11060-014-1668-y
24. DS R (1977) Pathology of tumors of the nervous system. Williams & Wilkins, Baltimore
25. Liu Z, Lv X, Wang W, An J, Duan F, Feng X, Chen X, Ouyang B, Li S, Singh S, Qiu S (2014) Imaging characteristics of primary intracranial teratoma. Acta Radiol 55:874–881. https://doi.org/10.1177/0284185113507824
26. Orakcioglu B, Halatsch ME, Fortunati M, Unterberg A, Yonekawa Y (2008) Intracranial dermoid cysts: variations of radiological and clinical features. Acta Neurochir (Wien) 150:1227–1234; discussion 1234. https://doi.org/10.1007/s00701-008-0152-x
27. Robles Fradejas M, Gonzalo García I, De Las Casas Quispe AC, Martin García A, García Higuera MI, Rodriguez Minguélez M, Martínez-Guisasola J (2017) Fetal intracranial immature teratoma: presentation of a case and a systematic review of the literature. J Matern Fetal Neonatal Med 30:1139–1146. https://doi.org/10.1080/14767058.2016.1205029
28. Georgiu C, Opincariu I, Cebotaru CL, Mirescu Ş C, Stănoiu BP, Domşa TA, Şovrea AS (2016) Intracranial immature teratoma with a primitive neuroectodermal malignant transformation - case report and review of the literature. Rom J Morphol Embryol 57:1389–1395
29. Fauchon F, Jouvet A, Paquis P, Saint-Pierre G, Mottolese C, Ben Hassel M, Chauveinc L, Sichez JP, Philippon J, Schlienger M, Bouffet E (2000) Parenchymal pineal tumors: a clinicopathological study of 76 cases. Int J Radiat Oncol Biol Phys 46:959–968. https://doi.org/10.1016/s0360-3016(99)00389-2
30. Mynarek M, Pizer B, Dufour C, van Vuurden D, Garami M, Massimino M, Fangusaro J, Davidson T, Gil-da-Costa MJ, Sterba J, Benesch M, Gerber N, Juhnke BO, Kwiecien R, Pietsch T, Kool M, Clifford S, Ellison DW, Giangaspero F, Wesseling P, Gilles F, Gottardo N, Finlay JL, Rutkowski S, von Hoff K (2017)

Evaluation of age-dependent treatment strategies for children and young adults with pineoblastoma: analysis of pooled European Society for Paediatric Oncology (SIOP-E) and US Head Start data. Neuro Oncol 19:576–585. https://doi.org/10.1093/neuonc/now234
31. Bisdas S, D'Arco F (2019) Pediatric Tumor Neuroradiology. In: Barkhof F, Jager R, Thurnher M, Rovira Cañellas A (eds) Clinical neuroradiology: the ESNR textbook. Springer International Publishing, Cham, pp 1–80
32. Komakula S, Warmuth-Metz M, Hildenbrand P, Loevner L, Hewlett R, Salzman K, Couldwell W, Lin CT, Osborn A (2011) Pineal parenchymal tumor of intermediate differentiation: imaging spectrum of an unusual tumor in 11 cases. Neuroradiology 53:577–584. https://doi.org/10.1007/s00234-010-0794-2
33. Fakhran S, Escott EJ (2008) Pineocytoma mimicking a pineal cyst on imaging: true diagnostic dilemma or a case of incomplete imaging?. AJNR Am J Neuroradiol 29:159–163. https://doi.org/10.3174/ajnr.A0750
34. Barboriak DP, Lee L, Provenzale JM (2001) Serial MR imaging of pineal cysts: implications for natural history and follow-up. AJR Am J Roentgenol 176:737–743. https://doi.org/10.2214/ajr.176.3.1760737
35. Gokce E, Beyhan M (2018) Evaluation of pineal cysts with magnetic resonance imaging. World J Radiol 10:65–77. https://doi.org/10.4329/wjr.v10.i7.65
36. Cauley KA, Linnell GJ, Braff SP, Filippi CG (2009) Serial follow-up MRI of indeterminate cystic lesions of the pineal region: experience at a rural tertiary care referral center. AJR Am J Roentgenol 193:533–537. https://doi.org/10.2214/ajr.08.1906
37. Bunin GR, Surawicz TS, Witman PA, Preston-Martin S, Davis F, Bruner JM (1998) The descriptive epidemiology of craniopharyngioma. J Neurosurg 89:547–551. https://doi.org/10.3171/jns.1998.89.4.0547
38. Zhou L, Li Q, Luo L, Xu J, Zhang Y, Chen T, Wei Y, You C (2009) Radiological features of craniopharyngiomas located in the posterior fossa. J Neurol Sci 287:119–125. https://doi.org/10.1016/j.jns.2009.08.012
39. Müller HL (2014) Craniopharyngioma. Endocr Rev 35:513–543. https://doi.org/10.1210/er.2013-1115
40. Lee IH, Zan E, Bell WR, Burger PC, Sung H, Yousem DM (2016) Craniopharyngiomas: radiological differentiation of two types. J Korean Neurosurg Soc 59:466–470. https://doi.org/10.3340/jkns.2016.59.5.466
41. Kane LA, Leinung MC, Scheithauer BW, Bergstralh EJ, Laws ER Jr, Groover RV, Kovacs K, Horvath E, Zimmerman D (1994) Pituitary adenomas in childhood and adolescence. J Clin Endocrinol Metab 79:1135–1140. https://doi.org/10.1210/jcem.79.4.7525627
42. Colao A, Loche S, Cappa M, Di Sarno A, Landi ML, Sarnacchiaro F, Facciolli G, Lombardi G (1998) Prolactinomas in children and adolescents. Clinical presentation and long-term follow-up. J Clin Endocrinol Metab 83:2777–2780. https://doi.org/10.1210/jcem.83.8.5001
43. Gold EB (1981) Epidemiology of pituitary adenomas. Epidemiol Rev 3:163–183. https://doi.org/10.1093/oxfordjournals.epirev.a036232
44. Perry A, Graffeo CS, Marcellino C, Pollock BE, Wetjen NM, Meyer FB (2018) Pediatric pituitary adenoma: case series, review of the literature, and a skull base treatment paradigm. J Neurol Surg B Skull Base 79:91–114. https://doi.org/10.1055/s-0038-1625984
45. Hwang J, Seol HJ, Nam DH, Lee JI, Lee MH, Kong DS (2016) Therapeutic strategy for cavernous sinus-invading non-functioning pituitary adenomas based on the modified Knosp grading system. Brain Tumor Res Treat 4:63–69. https://doi.org/10.14791/btrt.2016.4.2.63
46. Micko AS, Wöhrer A, Wolfsberger S, Knosp E (2015) Invasion of the cavernous sinus space in pituitary adenomas: endoscopic verification and its correlation with an MRI-based classification. J Neurosurg 122:803–811. https://doi.org/10.3171/2014.12.Jns141083
47. Simmons GE, Suchnicki JE, Rak KM, Damiano TR (1992) MR imaging of the pituitary stalk: size, shape, and enhancement pattern. AJR Am J Roentgenol 159:375–377. https://doi.org/10.2214/ajr.159.2.1632360
48. D'Ambrosio N, Soohoo S, Warshall C, Johnson A, Karimi S (2008) Craniofacial and intracranial manifestations of langerhans cell histiocytosis: report of findings in 100 patients. AJR Am J Roentgenol 191:589–597. https://doi.org/10.2214/ajr.07.3573
49. Aihara Y, Chiba K, Eguchi S, Amano K, Kawamata T (2018) Pediatric Optic Pathway/Hypothalamic Glioma. Neurol Med Chir (Tokyo) 58:1–9. https://doi.org/10.2176/nmc.ra.2017-0081
50. Fangusaro J, Witt O, Hernáiz Driever P, Bag AK, de Blank P, Kadom N, Kilburn L, Lober RM, Robison NJ, Fisher MJ, Packer RJ, Young Poussaint T, Papusha L, Avula S, Brandes AA, Bouffet E, Bowers D, Artemov A, Chintagumpala M, Zurakowski D, van den Bent M, Bison B, Yeom KW, Taal W, Warren KE (2020) Response assessment in paediatric low-grade glioma: recommendations from the Response Assessment in Pediatric Neuro-Oncology (RAPNO) working group. Lancet Oncol 21:e305–e316. https://doi.org/10.1016/s1470-2045(20)30064-4
51. Taylor T, Jaspan T, Milano G, Gregson R, Parker T, Ritzmann T, Benson C, Walker D (2008) Radiological classification of optic pathway gliomas: experience of a modified functional classification system. Br J Radiol 81:761–766. https://doi.org/10.1259/bjr/65246351
52. Freeman JL, Coleman LT, Wellard RM, Kean MJ, Rosenfeld JV, Jackson GD, Berkovic SF, Harvey AS (2004) MR imaging and spectroscopic study of epileptogenic hypothalamic hamartomas: analysis of 72 cases. AJNR Am J Neuroradiol 25:450–462
53. Delalande O, Fohlen M (2003) Disconnecting surgical treatment of hypothalamic hamartoma in children and adults with refractory epilepsy and proposal of a new classification. Neurol Med Chir (Tokyo) 43:61–68. https://doi.org/10.2176/nmc.43.61
54. Whitehead MT, Vezina G (2014) Interhypothalamic adhesion: a series of 13 cases. AJNR Am J Neuroradiol 35:2002–2006. https://doi.org/10.3174/ajnr.A3987
55. Siddiqui A, D'Amico A, Colafati GS, Cicala D, Talenti G, Rajput K, Pinelli L, D'Arco F (2019) Hypothalamic malformations in patients with X-linked deafness and incomplete partition type 3. Neuroradiology 61:949–952. https://doi.org/10.1007/s00234-019-02230-z

Publisher's Note Springer Nature remains neutral with regard to jurisdictional claims in published maps and institutional affiliations.